Green Synthesis of Reduced Graphene Oxide Nanosheet by using L-ascorbic Acid and Study of its Cytotoxicity on Human Cervical Cancer Cell Line

PRABHAT KUMAR, ANJANA SARKAR AND PURNIMA JAIN*

Department of Chemistry, Netaji Subhas University of Technology, New Delhi, India.

ABSTRACT

Biocompatible graphene derivative materials (GBMs) to harness the maximum potential of pristine graphene biologically, is the most important strategy for its advanced applications in pharmaceutical and other biomedical fields. Currently, scientists are trying to find this by using biopolymer nanocomposites or anchored materials. Nevertheless, tuning the bare GBMs towards biocompatibility is a beautiful approach to exploit the fundamental potential of pristine graphene vis-à-vis suppressing the effects of incorporated biopolymers or anchored materials. Herein, a large-scale, cost-effective, facile, and environment-friendly green synthetic strategy is used for the synthesis of reduced graphene oxide (rGO) nanosheet using L-ascorbic acid (L-AA) as a reducing/stabilizing/capping agent. The as-synthesized rGO was characterized by XRD, Raman spectroscopy, TEM, and in-vitro *cell cytotoxicity through SiHa (human cervical cancer) cell line. Results showed that nanosheet of rGO was synthesized successfully and the order of cell viability on SiHa cell line was found to be* $rGO_{ascorbic\ acid} > GO > rGO_{hydrazine}$*. The reason behind such viability order may be surface oxidation state, carbon content, and presence of reducing/surfactant/capping agent along with graphene. The studies described can be further optimized to be used in neural tissue engineering, regenerative medicines, biosensors, drug delivery, and gene delivery therapy, to name a few.*

KEYWORDS: *Reduced graphene oxide, Nanosheet, Ascorbic acid, Cytotoxicity; SiHa Cell line, Biomaterial.*

Highlights

- A systematic study was performed to synthesize, characterize, and to evaluate the cytotoxicity level of GO, $rGO_{hydrazine}$ and $rGO_{ascorbic\ acid}$ respectively.

J. Polym. Mater. Vol. **39,** No. 1-2, 2022, 121-135

*Correspondence author e-mail: erprabhatmtech@gmail.com; purnima.jain@nsut.ac.in
DOI : https://doi.org/10.32381/JPM.2022.39.1-2.8

- The study supports that L-Ascorbic acid acts as a green mild reducing agent vis-a-vis stabilizing agent/capping agent/surfactant for exfoliation and reduction of GO.
- Partially reduced graphene oxide successfully synthesized through L-ascorbic acid and the order of cell viability was found to ber$GO_{ascorbic\ acid}$> GO >r$GO_{hydrazine}$ against SiHa Cell line.
- Calculated EC_{50} was126.90 μg /ml (r$GO_{hydrazine}$), 132.98 μg/ml (GO), and 139.66 μg/ml (r$GO_{ascorbic\ acid}$) at 72 h.

1. INTRODUCTION

Graphene, a well-acclaimed established sp^2 hybridized 2D nanomaterials has not only opened the promising fundamental roles for forefront development of nanoelectronics[1], photonics[2], solar power harvesting[3], or flexible ultrathin nanodevice[4] but also showed its applications in biological systems. An interdisciplinary approach is required for the development of neural networks in tissues[5], regenerative medicines[6], or any biomaterial[7] with the successful establishment in biological systems[8]. Since the institutionalization of graphene by Nobel laureate Sir Andre Geim and Konstantin Novoselov in 2004, graphene-based nanomaterials have gained a lot of attraction due to their extraordinary electronic, optical, mechanical, chemical, and physical properties[9]. High electrical conductivity(10^6 siemens/m)[10], ultra-high theoretical electron mobility (10^5 cm^2/vs)[11], high visible transmittance (98%)[12] and excellent mechanical properties (about 1100 GPa)[13] make graphene a suitable candidate for applications as biomaterials.

Nevertheless, these properties can regulate neural interaction, adhesion, and mobility, as well as the capability to absorb aromatic biomolecules and selectively detect single-stranded DNA(ss DNA) through a π-π stacking interaction and/or electronic interaction by utilizing large surface area and sp^2 bonded carbon atoms in graphene[14]. Therefore, these materials have been considered as potential candidates in the research area of nanomedicine. Moreover, it would impact the human race positively by curing injury affecting the nervous tissues (e.g., Parkinson's, Alzheimer's, peripheral nerve loss, and spinal cord injury) by developing an advanced and more efficient neural network model[15-16].

However, the use of a safe range of concentrations as a biomaterial; its toxicity, and biocompatibility must be established to the permitted value[17]. Moreover, positive findings from functionalized derivatives of graphene with other nanoparticles[18] and nanogrids[19] as well as for neuron and astrocyte growth for neurogenesis[20] in the nervous system and in the regeneration of vital organ like bones, liver, lungs and kidney, ear, nose, pancreas, to name a few, escalate further investigation of these materials.

Pristine graphene being the most suitable candidate for bioelectroactive applications, but its commercial production is still limited. While graphene oxide can be synthesized chemically in large quantities, but the parental property of pristine graphene is lost due to oxidative stress

and conversion of sp^2 to sp^3 hybridization. Therefore, we decided to examine the partially reduced graphene oxide as a suitable candidate for biological systems considering intermediary between pristine graphene and graphene oxide structurally, physically and chemically.

Further, toxicity and biocompatibility are other parameters which must be considered to bring it into the clinical applications. Therefore, an alternate approach must be established for synthesis purpose which could overcome the conventional issues. Keeping all points mentioned above, we have decided to compare synthesis and characterizations of reduced graphene oxide through hydrazine monohydrate and L- ascorbic acid (L-AA)[21] separately, considering hydrazine is toxic and explosive[22] while L- AA is a non-toxic, naturally employed reducing agent in living systems as well as in the laboratory[23]. Additionally, Changyan et al., mentioned that reduced Graphene oxide through L-AA could achieve a high C/O ratio and electrical conductivity comparatively[24]. The main aim of this experiment was to find out the threshold concentration of ascorbic acid reduced GO which can be incorporated to biopolymer to be used as a biomaterial. Here, we have synthesized graphene oxide through the modified Hummer method and reduced it further with hydrazine monohydrate and L-ascorbic acid separately. We have investigated its toxicity effects on SiHa (human cervical cancer) cell line which confirmed that ascorbic acid reduced graphene oxide is less toxic than hydrazine even in large dosage (EC_{50} = 139.66 µg/ml, 72 h) and hence this dosage can be considered as a novel outcome and can be used it in preclinical biological systems.

2. EXPERIMENTAL

2.1. Chemicals

Graphite powder (purity, 98% C, 50 mesh) was purchased from SRL, Maharashtra, India. L-(+)-ascorbic acid (99%) powder, dietary supplement was purchased from pharmacy shop of Hollywood secrets company, India and hydrazine monohydrate ($H_4N_2.H_2O$, 98%), hydrochloric acid (HCl), sulfuric acid [H_2SO_4, (98%)], hydrogen peroxide [H_2O_2 (30%)] were procured from Merck, India. Potassium permanganate ($KMnO_4$) and sodium nitrate ($NaNO_3$) were procured from Fisher Scientific, India. Dimethyl sulfoxide and 3(4,5-dimethyl thiazole-2-yl)-2,5-diphenyl tetrazolium bromide) (MTT) the assay was purchased from Sigma Aldrich, USA, and was used without further purification. RPMI-1640, FBS, trypsin, and antibodies were purchased from GIBCO Grand Island, New York, USA. Pure milli-Q water was used as and when required throughout the experiment.

2.2. Preparation of Graphene Oxide (GO)

A dispersed solution of GO was synthesized by the modified Hummer's method.[25] Graphite powder (4 g) and $NaNO_3$ (4g) in 200 ml of H_2SO_4 (98%) in a 1000 ml beaker were kept under an ice bath (0- 5°C) and stirred continuously for 24 h. $KMnO_4$ (24g) was added very slowly to keep temperature less than 10°C to avoid explosion and left overnight with continuous stirring. 400 ml of milli-Q water was added slowly and left for two hours with continuous stirring. The ice bath was removed and further left for 4 hours with continuous stirring. A brown color solution was obtained after heating the solution to 90°C for 30 minutes and left for 4 hours with continuous stirring at room temperature. 200 ml of 30 % H_2O_2 was added slowly for oxidation, a light-yellow color appeared. 400 ml of milli-Q water was taken in another beaker and the obtained solution was mixed and further stirred both the beakers for 2 hours. Stirring speed was fixed at 600 rpm in every case mentioned above. Both the beakers were kept overnight to let it settle down. Impurities were removed by washing the solid sample with 5% HCl and milli-Q water several times (neutral pH) with ultrasonication at every step for exfoliation to graphene oxide. The obtained gel-like quasi-solid material was dried at 60°C

in a vacuum oven for 24 h. Sample was sent for further characterizations.

2.3. Preparation of reduced graphene Oxide (rGO)

A dispersed solution of GO was prepared by dissolving it in milli-Q water (0.1 mg/ml) and ultrasonicated it at 20kHz and 80 W for 2 h. 1g of L- ascorbic acid (reducing agent) was added to 1000 ml of as-prepared GO solution with continuous stirring (@600 rpm) at 80°C for 24 h. NH_3 solution (25% w/w) was added to the medium to maintain pH ~ 10 to promote colloidal stability through the electrostatic repulsion. After being ultrasonicated for 30 min., the solution was kept for 2 h to settle. The obtained suspension was centrifuged at 2000 rpm for 30 min and washed with milli-Q water several times (neutral pH) and put in a vacuum oven at 60°C for 24 h. The same experiment was repeated by replacing ascorbic acid with hydrazine monohydrate of 1g. The sample was sent for further characterizations.

2.4. Cell culture and MTT assay studies

The cytotoxicity was studied using SiHa cell line (human cervical cancer) procured from the NCCS (National Centre for Cell Science), DBT, Pune, India. The reduced tetrazolium salt in the MTT (Methyl Thiazolyl Tetrazolium salt) assay was examined for cell viability and proliferation with the development of purple color formazan crystals. The cells were preserved in a humidified incubator (37°C, 5% CO_2) and grown with 1 mmol/L sodium pyruvate, 10% (v/v) fetal bovine serum (FBS), and antibiotics (streptomycin 10 μg/mL, penicillin 100 μg/mL) as monolayer in RPMI-1640 medium.[26] In a 96-well plate, SiHa cells (5000 cells/well) were grown and kept for 24 h. After that, varied concentrations of GO, $rGO_{hydrazine}$, and $rGO_{ascorbic\ acid}$ (12.5 - 200 μg) dissolved in fresh RPMI-1640 media were added to the different grown cells in 96 wells. The formed system was kept for 24 h, 48 h, and 72 h separately. 20 μl of MTT (5 mg/ml) was added in each well before four hours to complete the incubation period. To dissolve the formazan, 200 μl of DMSO was added to each system after removing the media after completion of the incubation period. The system was again left to grow for 10 min at room temperature. Positive control and blank were used in the experiment.

2.5. Characterizations

Synthesized samples were characterized by using X-ray diffraction (XRD), Raman spectroscopy,

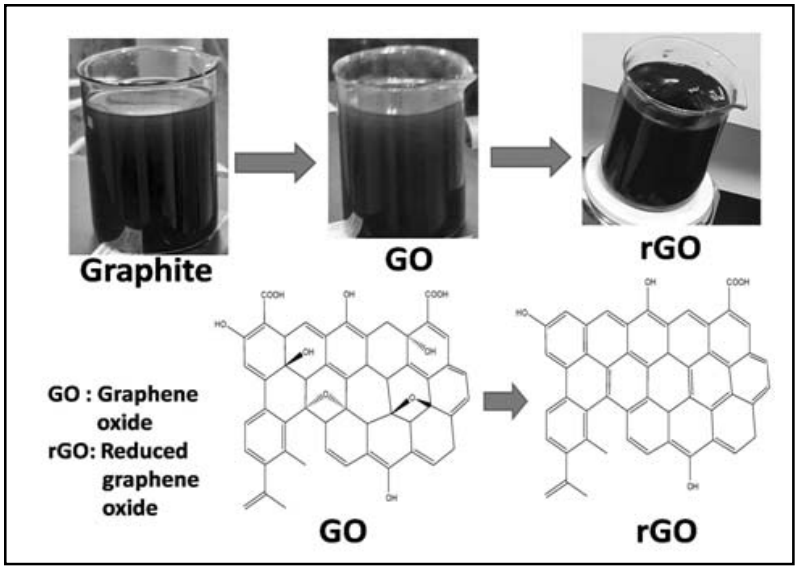

Scheme 1. Steps involved in the synthesis of reduced graphene.

transmission electron microscopy (TEM), high-resolution transmission electron microscopy (HR-TEM) & selected area electron diffraction (SAED) pattern. The XRD measurements were performed on powdered samples of graphite, GO and rGO using PAN alytical Xpert Pro system diffractometer (45 kV, 40 mA) with Cu Kα radiation (λ = 1.54178 Å). The relative intensities were recorded in the scattering range of 07°–70° (2θ) with a step of 2° min^{-1}. Raman measurements were performed from 500 to 3500 cm^{-1} at room temperature using Raman spectrometer (WiTec α-300 R, Germany) with an SSD laser excitation source (532 nm) at 5 mW applied voltage and 50x magnification objectives. The morphology of the GO and rGO sample was characterized through a transmission electron microscope (TEM JEOL-2100F). The sample was dispersed in water (1 mg/ml) through ultrasonication for 5 min and drop cast on a 200-mesh carbon-coated TEM grid. Cytotoxicity of samples was evaluated on SiHa cell line (human cervical cancer) using Bio-Rad microplate reader at 595 nm spectral wavelength.

3. RESULTS AND DISCUSSION

3.1. X-ray diffraction (XRD) analysis

Crystallinity, composition, and interlayer distance (d-spacing) of nanomaterials were determined by the analysis of obtained XRD patterns[27]. Figure. 1, shows the diffraction patterns of GO and rGO samples reduced through hydrazine monohydrate and ascorbic acid respectively. The well-defined peak (002) of graphite powder was obtained at 2θ ~ 26.71°, the interlayer distance (d-spacing) ~ 3.33 Å (JCPDS Card No.- 01-075-1621). As-prepared GO showed at 2θ ~ 11.7°, suggesting the oxidation of graphite with d-spacing ~ 7.60 Å through the induction of oxygen as epoxy, hydroxyl, and carboxyl functional groups on the surface of graphitic layers.[28] The expansion in graphite layers is due to intercalation of oxidizing agents and can be inferred through broader peak of GO than the main peak of graphite, leads to the deterioration of the crystal structure.[29] Higher d-spacing for GO in comparison to graphite indicates higher order of intercalation and oxidation of graphite.

Further, the oxygen functional groups are successfully removed from GO after its reduction which can be deduced along the disappearance of peak of GO in both the rGO samples and a broad peak appeared at 2θ ~ 26.2° in case of hydrazine hydrate and 2θ ~ 24.3° in case of ascorbic acid. Ascorbic acid can act as a better surfactant and stabilizing agent to keep layers dispersed which is further supported by the higher interlayer distance of $rGO_{ascorbic\ acid}$ (d = 3.60 A) than graphite powder (d = 3.33A) and $rGO_{hydrazine}$ (d = 3.40 Å).[30] This information accredits to the exfoliated rGO sheets within the poly hydrocarbon template and re-establishment of the sp^2 network.[31] The diffraction patterns were processed using Origin Pro 8 software via Gaussian curve fitting. The Bragg's equation was applied for calculating interlayer distance, d. The Scherer's equation with a constant equal to 0.9 was used for calculating the total height of the stacking layers, D in crystallites. The number of graphene layers in total crystallites sizes are depicted in Table 1.

3.2. Raman spectroscopy

Raman spectroscopy is a non-invasive technique extensively used to investigate the layered structure and disorders in graphene and its derivatives[32]. The positions of Raman peaks, shape, and intensity ratios provide categorical statistics about the number of layers and defects (edges, vacancies, ripples, etc.) present in the graphene lattice. Raman spectra of the GO and different rGO obtained in the

Table 1: Comparison of structural parameters deduced from the XRD patterns.

Peak (002)					
	2θ	**d(nm)**	**FWHM**	**D(nm)**	**n**
Graphite	26.71	0.333	0.4288	19.05631	57.226163
GO	11.7	0.760	1.95009	4.09827	5.39246029
rGOasc	24.3	0.360	8.7222	0.932396	2.58998854
rGOhyd	26.2	0.340	8.0762	1.010723	2.97271535

Notation: D— total height of stacking layers in crystallites, n—average number of graphene layers in graphene stacking nanolayers, d—average distance between graphene layers.

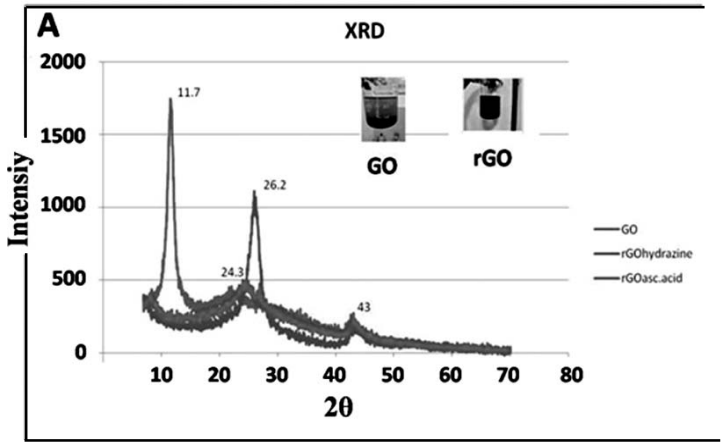

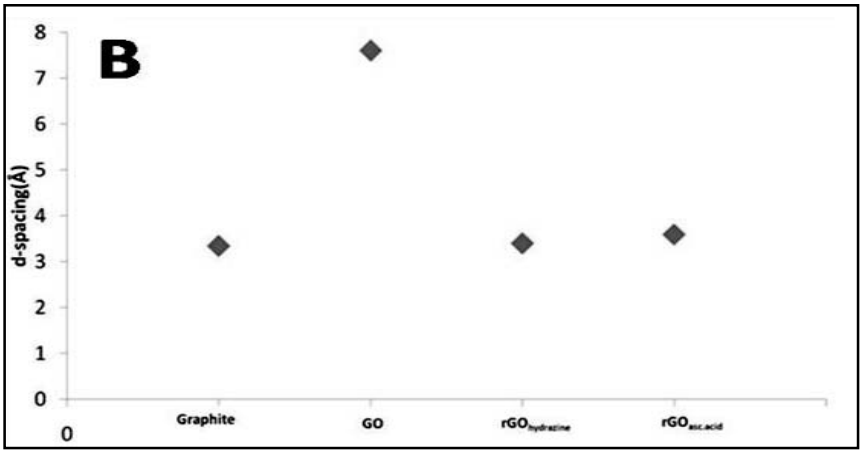

Figure. 1. XRD pattern of (A) GO, $rGO_{asc.\ acid}$, $rGO_{hydrazine}$(B) Interlayer Distance (d-spacing).

wavenumber range 900 cm^{-1} - 3400 cm^{-1} range at room temperature are shown in Figure 2. The D-band ~ 1350 cm^{-1} and the G-band ~ 1580 cm^{-1} and a wide hump with two broad peaks at the high wavenumber end (2700 cm^{-1}- 2900 cm^{-1}) correlate with the 2D band and 2D2 band is observed. The G-band originates due to (i) the sp^2 hybridized *C=C* bond stretching, and (ii) the Brillouin zone occupied by the first-order induced scattering from the doubly generated E_{2g} phonon.[33] Therefore, G-band carries detailed information about the sp^2 hybridized carbon network. In contrast, the origin of the D-band is related to the breathing mode of the aromatic rings which is due to excitation of charge carrier and its inelastic scattering by a phonon, second elastic scattering by defects due to oxygen-based functional groups in the carbon basal plane which results in recombination.[34] D-band, therefore, measures the degree of defects. The presence of 2D and 2D2 bands centered around 2700 cm^{-1}- 2900cm^{-1} is an overtone of the D band and also due to the double resonance transitions. The I_D/I_G ratio indicates the structural defects while 2D/G and 2D2 /G represent the number of layers[35] and better graphenization[36] respectively within the as-synthesized sample.

Although Raman spectra of all the three samples resemble identical in shape the intensity of Raman bands are obtained differently after oxidation/reduction and sonication processes. The Raman peaks and band intensity ratios obtained in various samples are listed in Table 2. After comparison, I_D/I_G ratio was observed in the order of $rGO_{hydrazine}$ < GO <$rGO_{ascorbic\ acid}$, which suggests a better formation of sp^2 hybridized carbon network. Indeed, ascorbic acid is a natural organic matter (NOM) which helps in the formation of more stable and dispersed graphene layers while hydrazine is a kind of charged inorganic material, promotes instability to graphene layers. Therefore, it can be concluded that L-AA is a more effective reductant than hydrazine for GO to obtain biocompatible rGO. Moreover, two other bands were observed around 2700 cm^{-1} and 2900 cm^{-1}, where the 2D band (2700 cm^{-1}) suggests the number of graphene layers. Here, the broadened and less intense band signifies that synthesized graphene holds few layers with some defects. Another band, 2D2 (2900 cm^{-1}), is a second-order peak that is obtained from the D-G band combination. The intensity ratio difference $I_{2D2}/I_G < I_{2D}/I_G$ attributed to the less oxygen content accompanied by fewer defects in graphene. The intensities of both peaks (D and G bands) increased in the case of $rGO_{hydrazine}$ and $rGO_{ascorbic\ acid}$ relative to GO, indicating a better-graphitized structure. However, the 2D/G and 2D2 /G intensity ratios are less than 1 in all the three samples suggests fewer layered and less graphenized structures.

TABLE 2. Raman bands of GO, $rGO_{asc.\ acid}$ and $rGO_{hydrazine}$

Sample	D Band	G Band	2D Band	2D2 Band	I_D/I_G	I_{2D}/I_G	I_{2D2}/I_G
GO	1346	1587	2700	2900	1.18	0.077	0.04
$rGO_{ascorbic\ acid}$	1343	1586	2700	2900	1.25	0.21	0.04
$rGO_{hydrazine}$	1344	1586	2700	2900	1.03	0.30	0.04

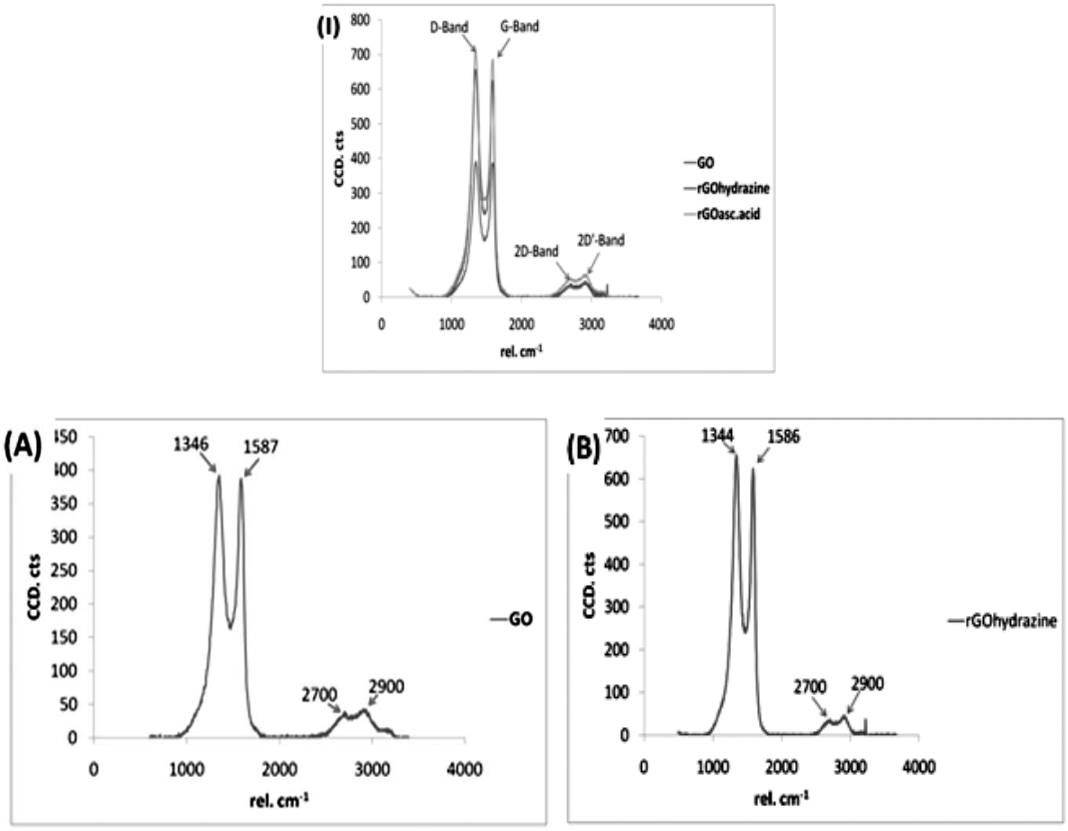

Figure 2. Raman band of (I) Overlapped and Zoomed view of (A) GO, (B) $rGO_{hydrazine}$ and (C) $rGO_{asc.acid}$.

3.3. Transmission electron microscopy (TEM) & Selected Area Electron Diffraction (SAED) pattern analysis

HR-TEM image and Selected Area Electron Diffraction (SAED) pattern were used to analyze the morphology and crystalline nature of the synthesized GO, $rGO_{hydrazine}$, and $rGO_{ascorbic\ acid}$ respectively as shown in Figure 3. The TEM results project the sheet-like structures in layers with Bernal stacking.[37] It is of mention here that by increasing the sonication time and optimizing the amount of reducing agents, these

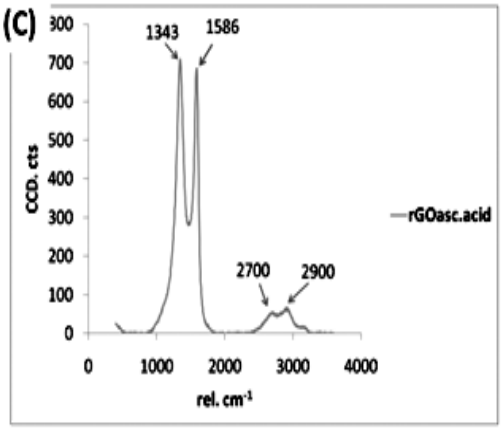

types of Bernal stacked multilayers could be further exfoliated and more monolayer graphene could be obtained. The better sheet-like morphology is high in the GO and a reduction/ breaking in sheet length is found with stronger reducing agents. Nevertheless, nanosheets are approximately 10 µm in length even after the use of reducing agents which are in accordance for making better electrical conduction coupled with electrically active biomolecules. The final results of the TEM observations are in agreement with XRD results and further suggest that the nanosheets dimension, morphology, and transparency can be tuned by optimizing capping/ oxidizing/reducing agents and the ultrasonication strategy for exfoliation.

The inset of corresponding TEM images shows the SAED pattern, as can be seen in Figure 3. In the case of the SAED pattern of GO, it is inferred that both amorphous, as well as crystalline regions, are present. The reason behind the formation of amorphous GO was the defects created by structural changes because of the formation of several sp^3 carbon atoms in the lattice. While in the case of $rGO_{hydrazine}$, the observed SAED patterns suggest more crystallinity than rGO ascorbic acid and GO due to the strong reducing nature of hydrazine than ascorbic acid.

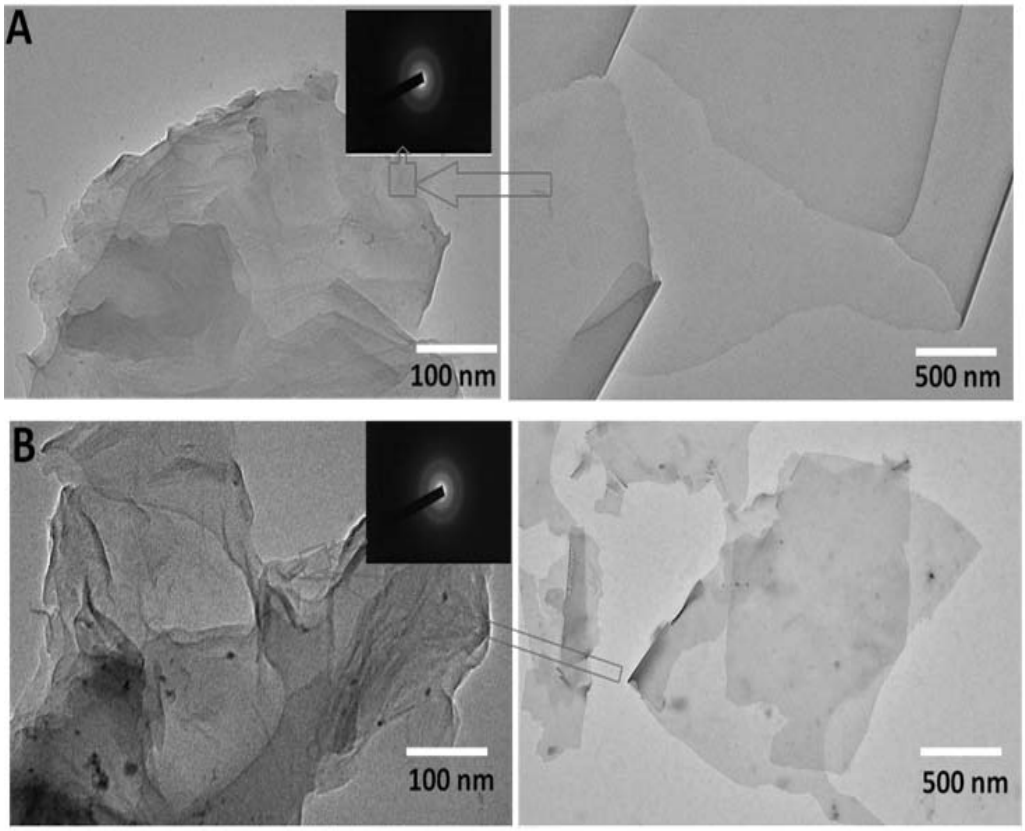

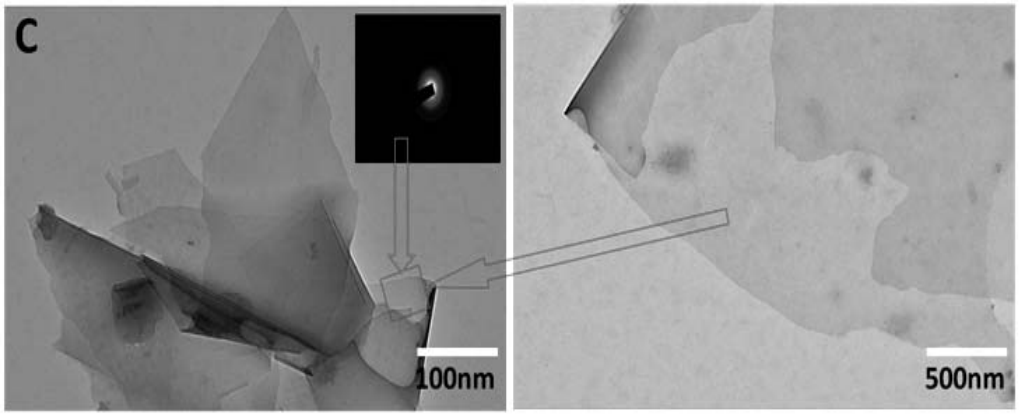

Figure 3. HR-TEM images and SAED Patterns of (A) GO, (B) $rGO_{Hydrazine}$ and (C) $rGO_{Asc.\ acid}$

4. Cytotoxicity

The cell viability, % was calculated using the following formula:

$$\% \text{ viability} = \frac{\text{(Mean Optical Density of treated cells)}}{\text{(Mean Optical Density of untreated cells, control)}} \times 100$$

In Panels of Figure 4, a comparative study of cell viability is performed on SiHa cell line. It was observed that the cell viability increases in the order of $rGO_{hydrazine}$ < GO < $rGO_{ascorbic\ acid}$ for 24 h, 48 h, and 72 h vis-a-vis for increased concentration of GO and rGOs (12.5-200 μg). EC_{50} computation was allowed only in the case of 72 hours exposure and was 126.90 μg /ml ($rGO_{hydrazine}$), 132.98 μg/ml (GO), and 139.66 μg/ml ($rGO_{ascorbic\ acid}$) are shown graphically in Figure 5. Our observations are in line with the

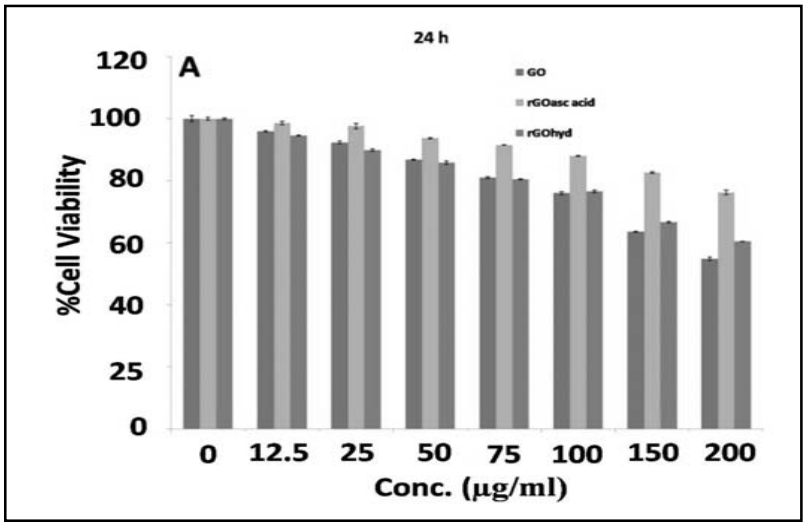

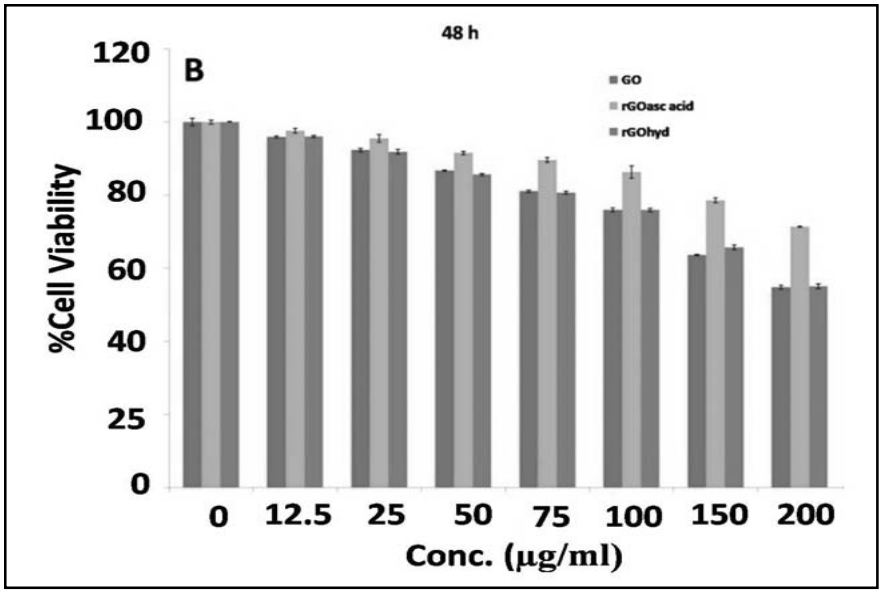

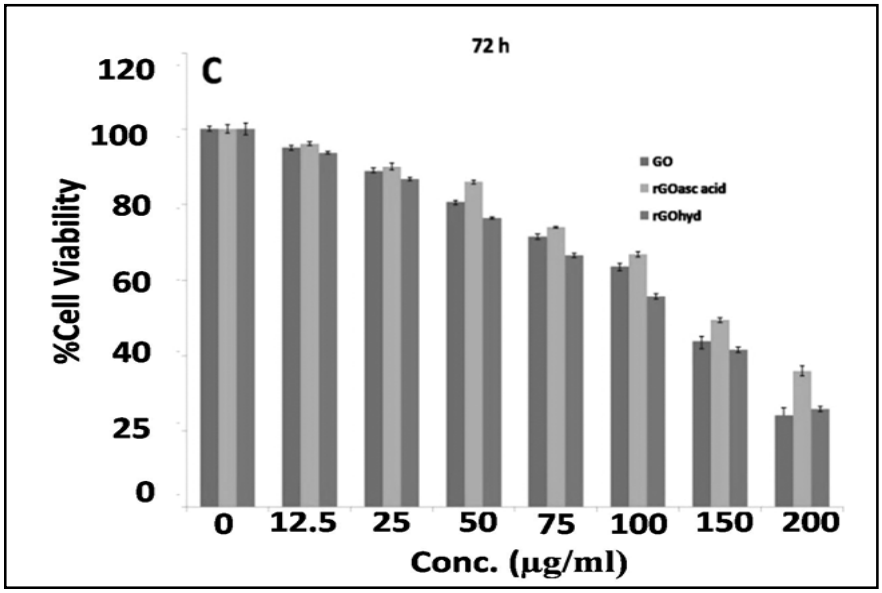

Figure 4. % Viability of SiHa cells treated with different concentration of GO, $rGO_{hydrazine,}$ and $rGO_{asc.\ acid}$ (A) 24 h (B) 48 h (C) 72 h.

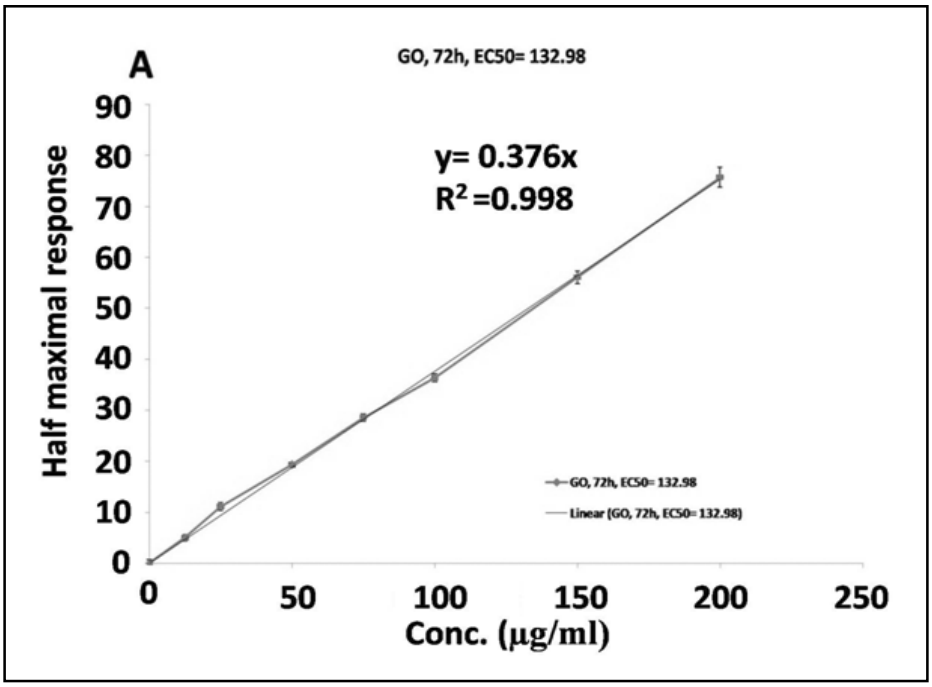
A
GO, 72h, EC50= 132.98
y= 0.376x
R2 =0.998
Half maximal response
Conc. (µg/ml)
GO, 72h, EC50= 132.98
Linear (GO, 72h, EC50= 132.98)

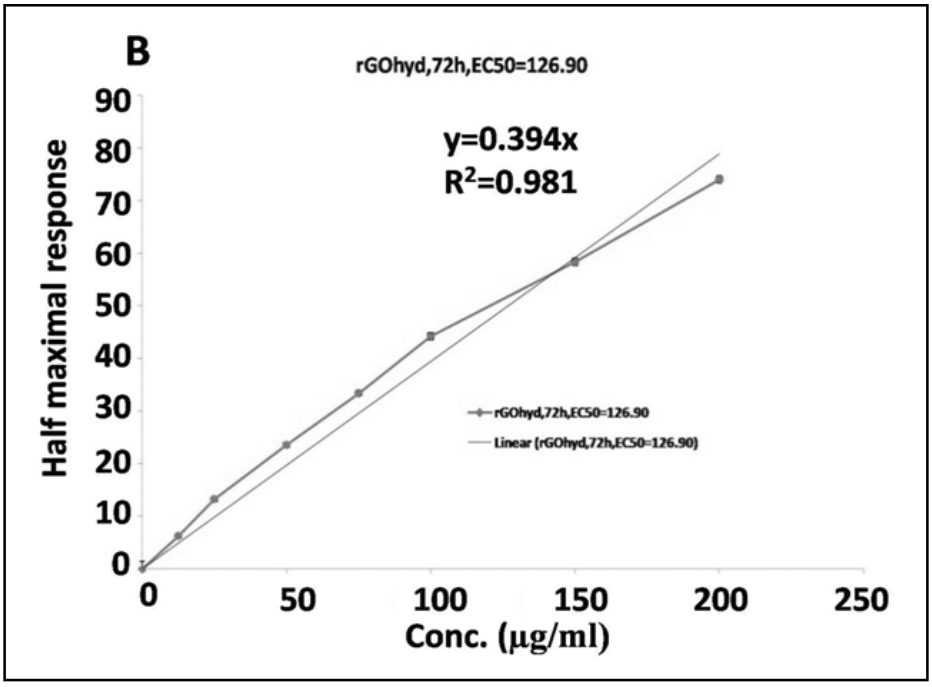
B
rGOhyd,72h,EC50=126.90
y=0.394x
R2=0.981
Half maximal response
Conc. (µg/ml)
rGOhyd,72h,EC50=126.90
Linear (rGOhyd,72h,EC50=126.90)

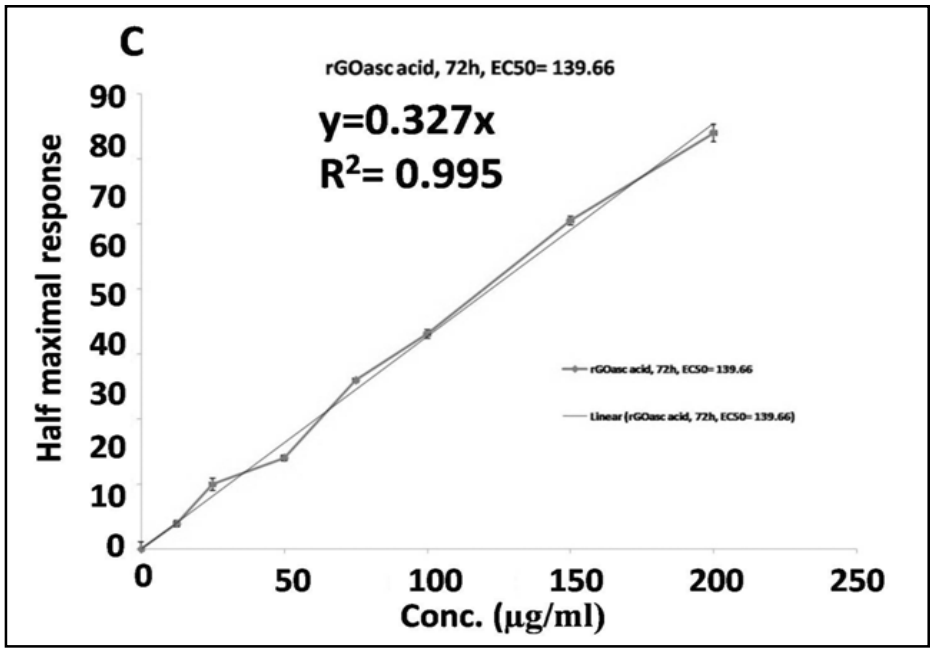

Figure 5. EC_{50} value of (A) GO (B) $rGO_{hydrazine}$ and (C) $rGO_{asc.\ acid}$. at 72 h.

previous studies demonstrating the cytotoxicity effect of GOs and rGOs of different concentrations.[38,39] The higher % cell viability in the case of $rGO_{asc.acid}$, could be due to different synthesis procedures, its size, shape, and antioxidant nature with non toxic behaviour.[40] Thus, preferably L-AA reduced GO can be considered as a suitable candidate in biological system than toxic hydrazine reduced GO. Therefore, from the in vitro cytotoxic study, it could be concluded that $rGO_{ascorbic\ acid}$ is far less toxic and sometimes favors increased cell viability due to the non-toxic and antioxidant nature of ascorbic acid which supports rGO towards less toxicity. Hence, further, it can be used as a biomaterial for targeted drug delivery, tissue engineering, neural network formation, etc. with optimized morphology, size, composition, and concentration.

CONCLUSION

In summary, a systematic study was performed to synthesize, characterize, and to evaluate the cytotoxicity level of GO, $rGO_{hydrazine}$, and $rGO_{asc.\ acid}$ respectively. The HR-TEM image confirms the formation of nanosheet of GO and rGOs in various conditions which could be well correlated with Raman peaks and SAED patterns. XRD pattern showed that GO and rGOs were synthesized successfully where $rGO_{asc.\ acid}$ has a broader and lesser intense 2θ peak than $rGO_{hydrazine}$, as d spacing between layers are more in the case of rGO using ascorbic acid (d = 0.360 nm) than hydrazine (d = 0.340 nm). This confirms that ascorbic acid is acting as a mild reducing agent as well as better stabilizing agent than hydrazine hydrate. In HR-TEM images, layers stacking

and breaking of nanosheets are lesser in the case of ascorbic acid while it is more in case of hydrazine, which signifies ascorbic acid as a better reducing agent/capping agent/ surfactant/stabilizing agent to form rGO nanosheet for biomaterial purposes. Raman bands confirms defect free exfoliation of graphite to graphene oxide and reduced graphene oxide while SAED pattern confirms its crystallinity. MTT assay studies against SiHa cell line confirmed that the toxicity level is in the order of $rGO_{hydrazine} > GO > rGO_{asc.acid}$ and it signifies that $rGO_{asc.\ acid}$ is less toxic even at the higher range of concentrations (EC_{50} = 139.66 µg/ml, 72 h) which can further be used in *in vivo* biological activity for tissue engineering, regenerative medicines, and targeted drug delivery, to name a few.

Acknowledgments

This work was financially supported by the Department of Chemistry, Netaji Subhas University of Technology, New Delhi. Prof. Jaydeep Bhattacharya, School of Biotechnology, Jawaharlal Nehru University, New Delhi is highly thankful for various discussions regarding the results part.

REFERENCES

1. X. Zhang, J. Qiushi, S. Ao, G. F. Schneider, D. Kireev, Z. Zhang and W. Fu, *Small,* 16 (2020): 1902820.
2. K. Amsaluand S. Palani, *Materials Today: Proceedings,* 33 (2020): 3372.
3. K. T. Lin, H. Lin, T. Yang, and B. Jia, *Nature communications,* 11 (2020): 1.
4. S. J. Heerema and C. Dekker, *Nature nano technology,* 11 (2016): 127.
5. D. Sood, K. Chwalek, E. Stuntz, D. Pouli, C. Du, M. T. Schomer, I. Georgakoudi, L. D. Black III and D. L. Kaplan, *ACS biomaterials science & engineering,* 2 (2016): 131.
6. S. Kumar, and K. Chatterjee, *ACS applied materials & interfaces,* 8 (2016): 26431.
7. E. Axpe, G. Orive, K. Franze and E. A. Appel, *Nature Communications,* 11 (2020): 1.
8. R.M. Marton and S. P. Pa'ca, *Trends in cell biology* 30 (2020): 133.
9. C. N. R. Rao, A. K. Sood, K. S.Subrahmanyam and A. Govindaraj, *Angewandte Chemie International Edition,* 48 (2009): 7752.
10. A. K. Geim and K. S. Novoselov, *Nanoscience and technology: a collection of reviews from nature journals*, (2010): 11.
11. K. S. Novoselov, A. K. Geim, S. V. Morozov, D. Jiang, Y. Zhang, S. V. Dubonos, I. V. Grigorieva and A. A. Firsov, *Science,* 306 (2004): 666.
12. K.S. Kim, Y. Zhao, H. Jang, S. Y. Lee, J. M. Kim, K. S. Kim, J. H. Ahn, P. Kim, J. Y. Choi and B. H. Hong, *Nature,* 457 (2009): 706.
13. I. A. Ovid'Ko, *Rev. Adv. Mater. Sci,* 34 (2013): 1.
14. E.M. Pérez and N. Martín, *Chem. Soc. Rev.* 44 (2015): 6425.
15. G.Orive, E. Anitua, J. L. Pedraz, and D. F. Emerich, *Nat. Rev. Neurosci,* 10 (2009): 682.
16. R.F.Keep, Y. Hua and G. Xi, *The Lancet Neurology,* 11 (2012): 720.
17. C. Bussy, H. A. Boucetta and K.Kostarelos, *Accounts of chemical research,* 46 (2013): 692.
18. A.Solanki, S. T. D.Chueng, P. T. Yin, R. Kappera, M.Chhowalla and K.B. Lee, *Advanced materials,* 25 (2013): 5477.
19. O. Akhavan and E. Ghaderi, *Journal of Materials Chemistry B,* 1 (2013): 6291.
20. C. Defteralý, R. Verdejo, L.Peponi, E. D. Martín, R. M. Murillo, M.A. L. Manchadoand C. V. Abejon, *Biomaterials,* 82 (2016): 84.

21. J. Zhang, H. Yang, G. Shen, P. Cheng, J. Zhang and S. Guo, *Chemical communications,* 46 (2010): 1112.

22. A. Furst, R. C. Berlo and S. Hooton, *Chemical Reviews,* 65 (1965): 51.

23. M. J. F. Merino, L. Guardia, J. I. Paredes, S. V. Rodil, P. S. Fernandez, A. M. Alonso and J. M. D. Tascon, *The Journal of Physical Chemistry C* 114 (2010): 6426.

24. C. Xu, X. Shi, A. Ji, L. Shi, C. Zhou and Y. Cui, *PloS one* 10 (2015): 0144842.

25. W. S. Hummers Jr and R. E. Offeman, *Journal of the american chemical society* 80 (1958): 1339.

26. U. Riaz, S. Jadoun, P. Kumar, R. Kumar and N. Yadav, *RSC advances,* 8 (2018): 37165.

27. C. F. Holder and R. E. Schaak, *ACS Nano,* 13 (2019): 7359.

28. A. M. Dimiev and J. M. Tour, *ACS Nano,* 8 (2014): 3060.

29. D. R. Chowdhury, C.Singh and A. Paul, *RSC Advances,* 4 (2014): 15138.

30. I. Chowdhury, M. C. Duch, N. D. Mansukhani, M. C. Hersam and D. Bouchard, *Environmental Science & Technology,* 47 (2013): 6288.

31. I. Chowdhury, N. D. Mansukhani, L. M. Guiney, M. C. Hersam and D. Bouchard, *Environmental Science & Technology,* 49 (2015): 10886.

32. A. C. Ferrari, *Solid state communications,* 143 (2007): 47.

33. J. C. Meyer, A. K. Geim, M. I. Katsnelson, K. S. Novoselov, T. J. Booth and S. Roth, *Nature,* 446 (2007): 60.

34. A. C. Ferrari, J. C. Meyer, V. Scardaci, C. Casiraghi, M. Lazzeri, F. Mauri, S. Piscanec, D. Jiang, K. S. Novoselov, S. Roth and A. K. Geim, *Physical Review Letters,* 97 (2006): 187401.

35. I. K. Moon, J. Lee, R. S. Ruoff and H. Lee, *Nature communications,* 1 (2010): 1.

36. C. Thomsen and S. Reich, *Physical review letters,* 85 (2000): 5214.

37. G. Jeong, B. Choi, D. S. Kim, S. Ahn, B. Park, J. H. Kang, H. Min, B. H. Hong and Z. H. Kim, *Nanoscale,* 9 (2017): 4191.

38. M. Pelin, L. Fusco, V. Leon, C. Martin, A. Criado, S. Sosa, E. Vazquez, A. Tubaro and M. Prato, *Scientific reports,* 7 (2017): 1.

39. S. Jaworski, E. Sawosz, M. Kutwin, M. Wierzbicki, M. Hinzmann, M. Grodzik, A. Winnicka, L. Lipinska, K. W³odyga and A. Chwalibog, *International Journal of Nanomedicine* 10 (2015): 1585.

40. S. Das, S. Singh, V. Singh, D.Joung, J. M. Dowding, D. Reid, J. Anderson, L. Zhai, S. I. Khondaker, W. T. Self, S. Seal, *Particle & Particle Systems Characterization* 30 (2013): 148.

Received: 22-03-2022

Accepted: 01-08-2022